Design of a High-energy, Two-stage Pulsed Plasma Thruster

T.E. Markusic[*] and **Y.C.F. Thio**[†]
Propulsion Research Center (PRC)
NASA Marshall Space Flight Center, Huntsville, AL 35812

J.T. Cassibry[‡]
University of Alabama in Huntsville, Huntsville, AL 35805

AIAA-2002-4125[§]

July 12, 2002

Design details of a proposed high-energy (∼50 kJ/pulse), two-stage pulsed plasma thruster are presented. The long-term goal of this project is to develop a high-power (∼500 kW), high specific impulse (∼7500 s), highly efficient (>50%), and mechanically simple thruster for use as primary propulsion in a high-power nuclear electric propulsion system. The proposed thruster (PRC-PPT1) utilizes a valveless, liquid lithium-fed thermal plasma injector (first stage) followed by a high-energy pulsed electromagnetic accelerator (second stage). A numerical circuit model coupled with one-dimensional current sheet dynamics, as well as a numerical MHD simulation, are used to qualitatively predict the thermal plasma injection and current sheet dynamics, as well as to estimate the projected performance of the thruster. A set of further modelling efforts, and the experimental testing of a prototype thruster, is suggested to determine the feasibility of demonstrating a full scale high-power thruster.

Nomenclature

C - thruster capacitance [F]
E - total discharge energy [J]
I_{bit} - impulse bit [N-s/shot]
I_{sp} - specific impulse [s]
Δv - maneuver velocity change [m/s]
η_t - thrust efficiency [%]
L_0 - initial thruster inductance [H]
L' - thruster inductance gradient [H/m]
m - mass [kg]
m_{bit} - mass bit [kg/shot]
L_A - anode length [cm]
L_C - cathode length [cm]
R_C - cathode radius [cm]

[*] Group Member, Fusion Propulsion, NASA/MSFC, Member AIAA.
[†] Leader, Fusion Propulsion, NASA/MSFC, Member AIAA.
[‡] Graduate Student Research Program Fellow, member AIAA.
[§] Presented at the 38^{th} AIAA Joint Propulsion Conference, Indianapolis, Indiana, July 7-10, 2002. Copyright by authors. Published by the AIAA with permission.

1 Introduction

Pulsed electromagnetic accelerators are devices which use intense bursts of electrical current ($\mathcal{O}(10^4 - 10^6)$ A) to create high speed ($\mathcal{O}(10^3 - 10^5)$ m/s) jets of plasma. They find application as plasma sources in many basic plasma science experiments[1] as well as in a specific genre of electric space propulsion device called the pulsed plasma thruster (PPT)[2]. The present work is motivated by the desire to improve the performance of pulsed electromagnetic accelerators in the context of plasma propulsion.

In what follows, the design of a proposed high-energy PPT is presented. The emphasis of the presentation is conceptual; this paper serves to define the principles of operation of the proposed thruster, provide rough calculations for the potential performance, and identify physical processes that will be the subject of future phenomenological modelling. We first provide a brief background of the state of PPT technology readiness – to serve as a backdrop for defining our motivation for pursuing the development of a new thruster.

1.1 Background

Modern PPTs have the potential for fulfilling the attitude control requirements on a satellite at greatly reduced mass and cost. They are also being considered for constellation maintenance for missions such as interferometric imaging of the Earth from space or deep space from an Earth orbit (c.f., Polzin *et al.*[3]). The benefits of PPTs are their simplicity, very small impulse bits for precise control of satellite motion, reliability, and high specific impulse. Two classifications of PPTs exist, corresponding to the form of propellant used: gas-fed (GFPPT) or ablative propellant (APPT). The gas-fed variety has the advantages of a "clean" exhaust plume and high specific impulse. The ablative version of the PPT uses a solid propellant, such as Teflon, to provide other advantages such as compactness and overall ease of system integration; however, plume contamination (with some solid propellants) and lower specific impulse may limit the application of APPTs for some missions.

From about 1960 to 1968 PPT research focused on the gas-fed variant (GFPPT). The GFPPT was envisioned as a potential "primary" propulsion system, where the GFPPT would process large amounts of power (>100 kW) and provide enough average thrust (>1 N) to perform large Δv maneuvers, such as interplanetary missions[4]. However, by the late sixties, research turned toward steady-flow electromagnetic acceleration (the MPD thruster). The quasi-steady MPD thruster[5] allowed for the amortization of efficiency-robbing losses intrinsic to pulsed operation (such as propellant loss at the leading and trailing edge of the gas injection pulse), through the use of a protracted current pulse and, hence, allowed for higher thrust efficiencies to be attained. A "secondary" propulsion niche, small Δv attitude control maneuvers, still existed for the GFPPT. However, at about the same time, the ablative variety of PPT (APPT) was gaining favor, mainly due to its mechanical simplicity. The GFPPT requires the storage of gaseous propellant under high pressure and a fast-acting valve to meter puffs of propellant into the discharge chamber. Further, the propellant feed system in the GFPPT is required to operate in a leak-free manner for many ($> 10^7$) shots. A flight qualified system capable of performing these demanding tasks was not available at the time and, hence, only APPTs were flown[6].

This state of affairs remained until the mid-90's, when the some of the negative issues related to propellant feeding in the GFPPT were ameliorated by the availability of more reliable valves and the development of high-speed solid-state electrical switching technology. The former development addressed the reliability issue, while the latter showed promise for substantially increasing the propellant utilization efficiency. These technologies were implemented in the thrusters of Ziemer *et al.*[7, 8, 9]. These low energy (<10 J) thrusters show promise for replacing APPTs in missions which require small Δv maneuvers. However, high-energy thrusters probably cannot benefit from the new switching technologies, since the necessarily high current levels preclude the use of solid-state switching devices.

Even with the addition of these new technologies, PPTs remain one of the least efficient electric propulsion systems (η_t <10%). However, the possibility of large incremental gains in performance make PPTs one of the most interesting devices, from a research perspective.

1.2 Motivation and Approach

No one type of thruster is best suited for all types of missions. For example, ion thrusters may be the best propulsion option for a large Δv, long duration mission; however, if short trip times are required, their characteristically low thrust density may preclude their use altogether. Similarly, Hall thrusters have attractive performance at intermediate specific impulse levels (∼2000 s), but fundamental physical limitations prevent them from achieving the high specific impulse levels required for some missions. In short, every type of electric propulsion device has a parameter space within which it performs best. It is our contention that the PPT may have unique capabilities to satisfy the propulsion needs for missions that require high specific impulse, high thrust efficiency, and high thrust density. The motivation of the present project is to develop a high power (∼500 kW), high specific impulse (∼7500 s), highly efficient (>50%) thruster for use as primary propulsion in a high power nuclear electric propulsion system. The thruster, which we call PRC-PPT1, uses a two-stage acceleration scheme, to circumvent some of the deficiencies which have plagued earlier thruster designs.

High-energy PPTs have already been experimentally shown[10] to be capable of accelerating current sheets to speeds greater than 150 km/s (corresponding to a specific impulse above 15,000 s, if 100% sweeping efficiency is assumed). Another study[4] demonstrated high-energy PPT operation at greater than 60% thrust efficiency (note: the efficiency was calculated using the estimated propellent mass inside the thruster during the current pulse; the cold-gas pulse was substantially longer in duration than the discharge and, hence, using the actual (total) cold-gas mass bit would have lead to a substantially lower calculated value of thrust efficiency). These experiments prove that there are no fundamental *physical* limitations that will prevent us from attaining our stated design goals. Let us state in one place, then, the *practical* limitations of past laboratory designs which must be addressed to bring high-energy PPTs to a level of maturity that will allow them to be considered as a viable near-term high-power electric propulsion option:

1. **Propellant utilization efficiency:** Two mechanisms contribute to low propellant utilization efficiency in gas-fed PPTs. As described earlier, the delivery of discrete gas puffs to the discharge chamber using mechanical valves is difficult. Ideally, a gas injection system would inject just enough gas to fill the discharge chamber and then quickly close. For typical thruster dimensions, a valve open-close duration of no more than about 100 μs is required to avoid propellant leakage after the electrical discharge pulse. The design of a mechanical valve to meet this specification is challenging. A second propellant loss mechanism in PPTs results from incomplete coupling of the Lorentz force density to the working gas. This inefficiency occurs when the accelerating current sheet is unable to fully entrain the propellant that it encroaches upon. Permeability of current sheets remains an active research topic[11].

2. **Electrical efficiency:** Typical PPTs suffer from poor electrical impedance matching between the source and the load. Oscillatory current waveforms result, which lead to undesirable "restrike" in the discharge chamber and significant energy dissipation inside the capacitor.

3. **Electrode erosion:** Lifetime-limiting electrode erosion remains a major issue in assessing the viability of high-power PPTs. Electrode erosion has been more extensively studied in steady-flow plasma thrusters[12]. There remains a need for an experimental database of electrode erosion rates for PPTs, using a variety of electrode materials, propellants, electrode temperatures, current levels, etc..

4. **Reliability:** The reliability (and lifetime) of high-power PPTs is impacted most strongly by the following components: the gas injection valve, the capacitors, the high current switch, and the (eroding) electrodes. New high-power PPT designs must address the reliability of each of these components, or somehow eliminate the need for them in the system.

The "issues" that have been enumerated above define the challenges that confront the development of a new thruster, that is, new thruster designs should strive to positively impact one or more of these PPT deficiencies. We now list, in a general sense, how our proposed thruster design addresses each of these points (details of the design will be given in subsequent sections):

1. **Propellant utilization efficiency:** PRC-PPT1 uses a *liquid* metal (lithium) feed system that requires no mechanical valve. Propellant loading is achieved through the vaporization and ionization of a liquid droplet (first stage); the size of the droplet is tailored to precisely deliver the desired propellant mass to the discharge chamber, where it is electromagnetically accelerated (second stage). Thus, problems associated with using a gaseous propellant feed system are eliminated. To address the propellant sweeping efficiency issue, PRC-PPT1 will operate in a higher gas density regime than is typical. Traditional PPTs have been plagued with poor efficiency, at least partially, because they have not been operated in a plasma regime that fully exploits the potential benefits of pulsed plasma acceleration by electromagnetic forces. PPTs have generally been used to accelerate low-density plasmas. Operation of thrusters in this plasma regime allows for the development of certain undesirable particle-kinetic effects, such as Hall effect-induced current sheet canting[13]. PRC-PPT1 was designed to propel a highly collisional, dense plasma that has more fluid-like properties and, hence, is more effectively pushed by a magnetic field[14]. Traditional PPTs also suffer from dynamic efficiency losses associated with "snowplow" loading of distributed neutral propellant. The two-stage scheme used in PPT-1 allows the propellant to be loaded in a manner which more closely approximates the optimal "slug" loading.

2. **Electrical efficiency:** PRC-PPT1 will use a toroidal "transmission line" capacitor. The custom-designed capacitor, similar to those developed by Hayworth *et al.*[15], will be impedance matched to the load (the thruster arc discharge) to yield a non-ringing current waveform, leading to more efficient transfer of the capacitively stored energy. The capacitor design will also lead to a smaller, lighter overall thruster design. The thruster discharge chamber will occupy the hollow central region of the capacitor; the use of a single, large capacitor of this design has been shown to be considerably lighter (one-sixth) than a conventional parallel combination of equal total capacitance[16]. Also, the thruster geometry has been chosen to maximize electrical efficiency. The

electrode configuration is designed to form a "virtual cathode" (see section 2.1), which will maximize the discharge chamber axial inductance gradient and, hence, increase the electrical efficiency[2].

3. **Electrode erosion:** PRC-PPT1 will use a hollow, truncated cathode (inner electrode). The aim is to distribute the cathode current over a larger area, prevent current constriction inside the electrode material (which occurs at the leading edge of a propagating current sheet), and to provide a plasma-electrode interface that is not starved of propellant. Lithium propellant was chosen, for among other reasons, to test whether or not the reduced electrode erosion found in the Lithium Lorentz Force Accelerator (LiLFA)[17] could also be realized in a pulsed plasma thruster.

4. **Reliability:** The use of the molten lithium plasma injector eliminates the need for both a gas valve and a high-current electrical switch (both the first and second stage are self-switching); the injector design fulfills both roles using no moving parts to provide, in principle, a highly reliable propellant feed and electrical switching system. The transmission line capacitor eliminates lifetime-limiting current reversal and includes an integrated cooling system to extend capacitor life.

The sections which follow more completely describe the geometry and operation of the proposed thruster, and present the preliminary design of a proof-of-principle laboratory thruster.

2 Thruster Description

2.1 General description

The PRC-PPT1 is a two-stage pulsed plasma thruster (the use of multi-stage electromagnetic acceleration was first advocated by Turchi *et al.*[18], who used a Teflon-ablative PPT to inject plasma into a second, electromagnetic accelerator stage). The components of PRC-PPT1 are schematically illustrated in Fig. 1.

The sequence of events in the operation of the thruster is as follows. Liquid lithium is delivered from a reservoir to the first stage using an MHD pump. A lithium droplet forms at the outlet of the propellant feed system, inside the first-stage plasma injector. A high current discharge initiates inside the injector, which vaporizes and ionizes the lithium droplet. The injector ejects a dense, thermal plasma into the main discharge cavity (second stage). A Townsend avalanche ensues, forming a current sheet with mega-amp level current. The current sheet accelerates the length of the second stage, entraining the propellant and ejecting it from the thruster at a speed on the order of 100 km/s.

Let us consider each of these phases of operation in more detail. The propellant feed system is diagrammatically illustrated in Fig. 2a. Liquid lithium propellant is stored in an un-pressurized, heated ($\sim$180 C°) reservoir. The propellant is delivered from the reservoir to the thruster using an MHD flow coupler[19]. The flow coupler applies a $\mathbf{J}\times\mathbf{B}$ force to the molten lithium by passing current through it, transverse to an applied magnetic field. Precise control of the lithium mass flow rate is accomplished by simply adjusting the current that passes through the flow coupler. The flow coupler has no moving parts – emphasizing an attractive feature of using a conductive propellant.

The lithium is fed into the first stage injector through a (electrically insulating) ceramic tube. The first stage capacitor is connected between the metal (stainless steel) lithium feed line and the outer electrode (anode) of the injector. As propellant is fed into the injector, a lithium droplet forms at the end of the ceramic feed line, as illustrated in Fig. 2b. As the droplet grows in size, it eventually contacts the outer electrode and "arcs-over" – closing the circuit connected to the first stage capacitor. The capacitor has sufficient energy to vaporize and (singly) ionize the entire lithium droplet. The newly formed lithium plasma thermally expands out of the first stage injector and into the second stage discharge chamber. The vaporization of the droplet re-opens the first stage capacitor circuit, allowing it to be recharged. As lithium is continuously being pumped by the flow coupler, a new droplet is formed and the process repeats. Again, two more advantages are gained through the use of a conductive propellant: no high current switch is needed in the first stage, as the circuit is self-switching, and the propellant in the feed line acts as the cathode, eliminating the first-stage cathode erosion issue. We are, in essence, feeding a liquid cathode into the injector, and using the cathode erosion products as the propellant for the second stage.

The final phase of operation in a single pulse of the PRC-PPT1 is the second stage electromagnetic acceleration. The conceptual (and, as yet, theoretically and experimentally unfounded) evolution of the second stage current sheet is envisaged in Fig. 3. The second stage electrode configuration, which is essentially a hybrid z-pinch/coaxial geometry, uses a truncated inner electrode (cathode) to induce a "virtual cathode" along the centerline of the accelerator, in an attempt to maximize the acceleration channel inductance gradient and, hence, max-

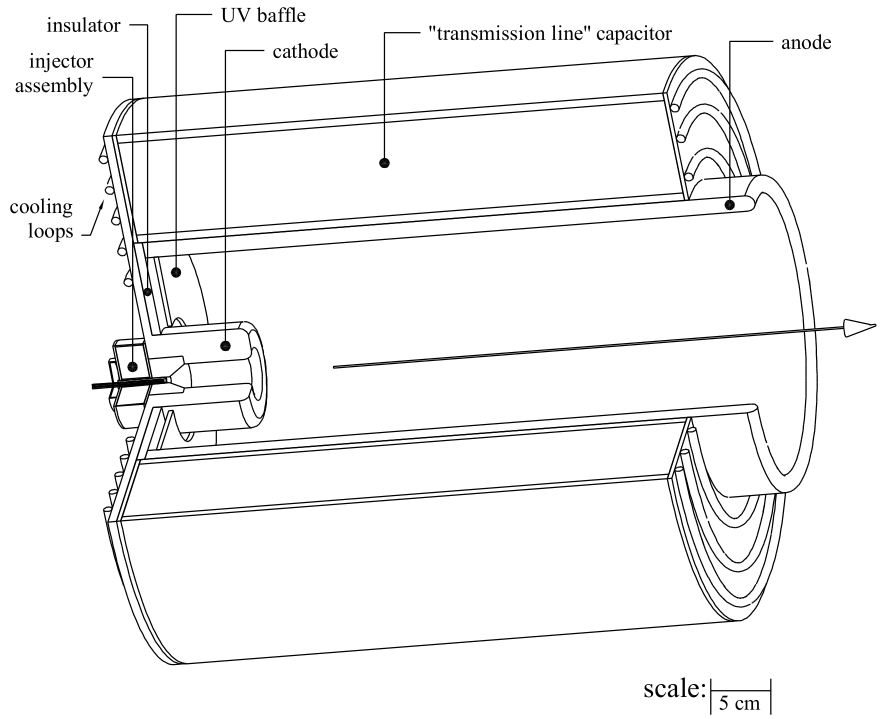

Figure 1: Schematic of the PRC-PPT1 geometry and components (sectioned to show inner detail).

imize the force on the current sheet. The current sheet is expected to initiate near the back of the accelerator – where the Poynting vector flux is first able to deposit its energy. The $\mathbf{J}\times\mathbf{B}$ force density will drive the current sheet around the end of the cathode, pinching the plasma at the center, in a manner similar to a dense-plasma-focus device[20]. Provided that current continues to be driven by the capacitor, the anode current sheet attachment will continue to propagate axially, and the cathode column will be extruded, forming a "virtual" center electrode (see Fig. 3c). The cathode current sheet attachment will distribute itself over the inside of the hollow cathode, conducting through residual lithium plasma from the first stage injector. The current sheet will continue to accelerate axially until the current subsides, either through exhaustion of the capacitively stored energy, or through the disruption of the virtual cathode column, from instabilities that are known to evolve in z-pinch current configurations. The entrained propellant will ultimately be ejected from the thruster, and thrust will be derived.

Other features of the PRC-PPT1 design are illustrated in Fig. 1. A metallic UV baffle is located in front of the breech insulator. The purpose of the baffle is to shield the insulator material from damaging ultraviolet radiation which is emitted from the current sheet plasma. Also shown are anode and cathode cooling loops. Both electrodes will be actively cooled using flowing liquid coolant.

The discussion above describes the general geometry and operation of the proposed thruster. The next section gives more specific design details for a first, proof-of-principle, thruster.

2.2 PRC-PPT1a design

The aim of our first experimental prototype thruster (PRC-PPT1a) is to validate the operation of the liquid lithium plasma feed system, to characterize the ejected plasma and test the repetitive operation of the first-stage plasma injector, and to map out the current sheet trajectory inside the second stage of the thruster – to see if the current sheet evolution envisaged in Fig. 3 can be realized in an actual thruster.

The design of the prototype thruster is constrained by several factors: first, of course, the thruster is expected to meet the performance goals stated in section 1.2, second, the components must be constructed from materials on-hand at the PRC and, lastly, the operation of the thruster must be compatible with vacuum facilities presently avail-

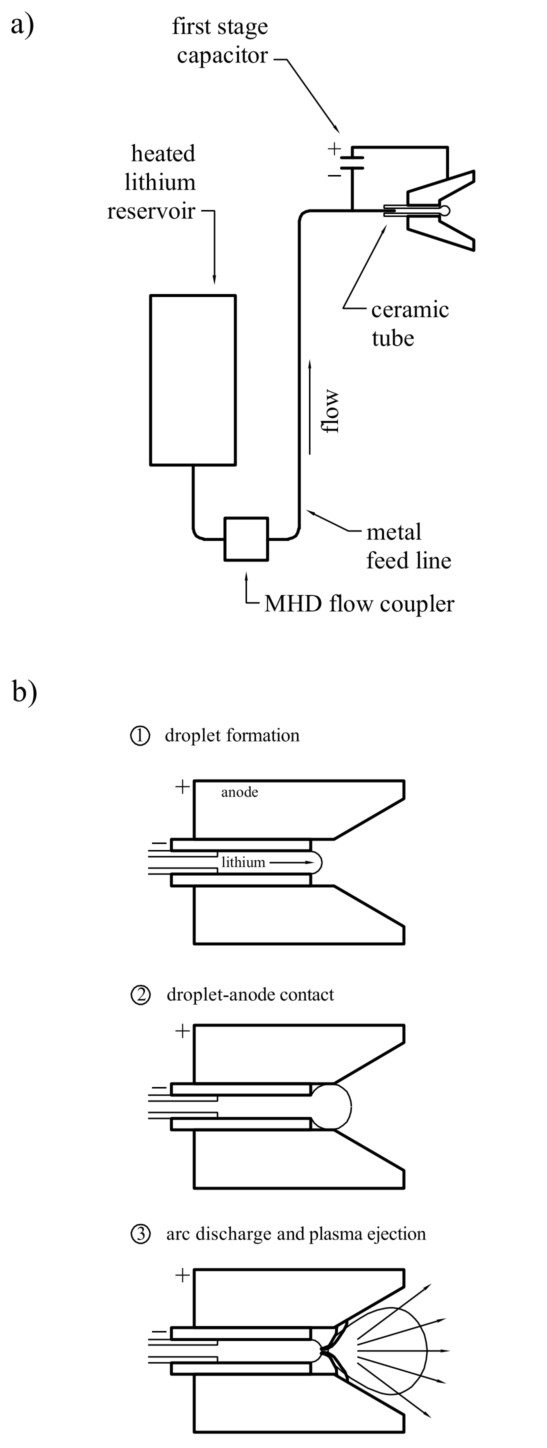

Figure 2: PRC-PPT1 propellant feed system: a) diagram of liquid lithium feed system, b) first-stage droplet formation and plasma ejection sequence.

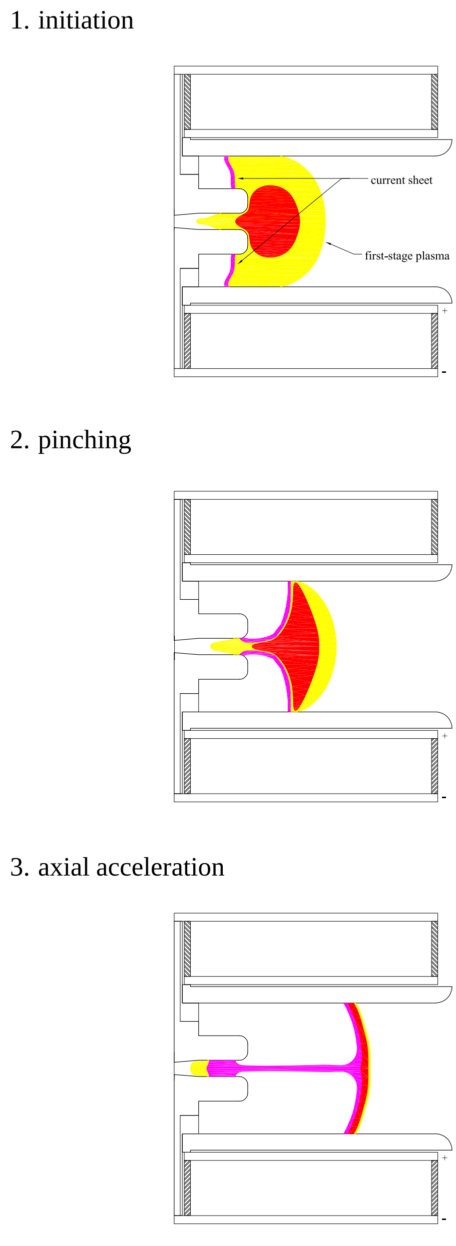

Figure 3: Conceptual evolution of current sheet in second stage of PRC-PPT1: initiation, pinching, and acceleration with virtual cathode.

able at the PRC. The last two constraints limit us to, at the present time, the design of a thruster that operates in a single shot mode, as we presently do not posses: capacitors suitable for repetitive operation, a high-power high-voltage power supply, or a vacuum facility capable of handling large mass flow rates. Components that are readily available in our laboratory inventory include 100 17.5 μF, 40 kV, low inductance (30 nH) capacitors, which were recently acquired from General Atomics Inc.. The capacitors have single ended coaxial connectors to facilitate low inductance connection to the thruster. A large selection of raw copper (including 20 cm diameter thick-walled pipe) material is available for use as electrode material.

A schematic illustration of the PRC-PPT1a complete assembly and a cross-section of the discharge chamber is shown in Fig. 4. The thruster will use four of the aforementioned capacitors, connected in parallel, to allow up to 50 kJ discharge energy. A cross-sectional schematic of the discharge chamber is shown in Fig. 4b, where the relevant dimensions are shown. In the illustration, only the anode inner radius is explicitly given; this is the dimension of the copper pipe that is available to us. The other dimensions, L_a, L_c, and R_c (the anode length, the cathode length, and the cathode radius, respectively) are to be established through modelling.

Since the dimensions of the thruster will be established through preliminary modelling efforts, let us list, in one place, the type of modelling efforts that will be needed to guide the physical dimensioning of the prototype thruster:

1. **Lithium droplet decomposition.** Modelling of the lithium droplet vaporization in the first stage plasma injector is necessary to predict the temporal evolution and thermodynamic state of the decomposition products, as well as to determine the first stage capacitor energy requirement. A model of the droplet formation itself will be necessary to size the first stage liquid injection orifice and electrode spacing.

2. **First stage injection.** The expansion of the first stage injector plasma should be modelled to guide the design of the injector and the second stage cathode. It is imperative that the first stage injector and second stage cathode deliver the majority of the lithium plasma propellant into the second stage discharge chamber before the second stage arc discharge commences, otherwise propellant will get left behind the accelerating current sheet and, hence, constitute a propellant utilization inefficiency. A 2-d fluid model would be helpful in estimating the temporal evolution of the lithium plasma density profile as it thermally expands out of the hollow cathode. A kinetic model will be required to accurately estimate the the time of breakdown.

3. **Current sheet propagation.** Modelling of the current sheet propagation is necessary to determine the proper length of the second stage anode. A 0-d current sheet/lumped circuit element model would provide a first estimate. A full 2-d MHD simulation would provide more accurate results, as well as elucidate the expected current sheet configuration, that is, show how the current sheet tilts as it propagates. This information could be used to tailor the first stage plasma injector to provide an initial mass distribution which inhibits adverse tilting of the current sheet.

4. **Stability of the virtual cathode.** The PRC-PPT1 design uses a hybrid z-pinch/coaxial electrode configuration, which is intended to produce a propagating planar current sheet electrically connected to the (physical) cathode at the back of the accelerator through a long plasma column (the virtual cathode). The virtual cathode is essentially a z-pinch current configuration, which is known to be unstable. For the purposes of the PRC-PPT1 design, a modelling effort, which draws upon existing knowledge, is needed to predict how long the virtual cathode can be maintained inside the accelerator, before current flow is disrupted by current driven instabilities. The onset of such instabilities may limit the length of the acceleration channel that can be practically be implemented.

As stated in the introduction, the present work is primarily conceptual in nature – the necessary modelling effort enumerated above has not been completed. To date, the first three items enumerated above have been addressed to a limited extent; the results of those efforts are presented in the next section.

3 Modelling

3.1 Current sheet propagation

A 0-d plasma thruster code (PTC1) was developed to obtain a rough estimate of the expected current sheet trajectory. The code is used to solve the unsteady thruster electrical circuit equations, coupled with a 1-d model of the current sheet dynamics. A schematic of the computational elements is shown in Fig. 5. The lumped circuit elements represent the following plasma thruster components:

C = capacitor capacitance
R1 = transmission line resistance
R2 = “crowbar” resistance
R3 = current sheet resistance
L1 = capacitor internal inductance
L2 = transmission line inductance
L3 = instantaneous thruster inductance

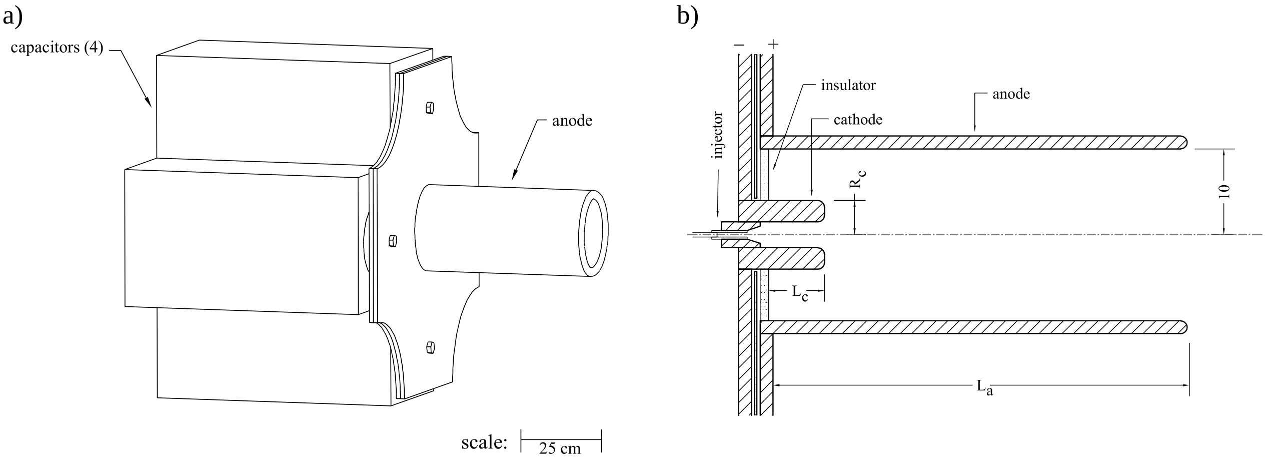

Figure 4: a) Isometric view of complete PRC-PPT1a assembly, b) Cross-section of PRC-PPT1a discharge chamber.

Applying Kirchoff's circuit laws and Newton's second law to the circuit illustrated in Fig. 5 results in five first-order simultaneous ODEs:

$$\dot{Q} = -I_1 \ , \tag{1}$$

$$\dot{I}_1 = \frac{1}{L_1 + L_2}\left[\frac{Q}{C} - (R_1 + R_2)I_1 + R_2 I_3\right] \ , \tag{2}$$

$$\dot{I}_3 = \frac{1}{L_3}\left[R_2 I_1 - (R_2 + R_3 + L'v)I_3\right] \ , \tag{3}$$

$$\dot{x} = v \ , \tag{4}$$

$$\dot{v} = \frac{1}{2m} L' I_3^2 \ , \tag{5}$$

where Q is the instantaneous charge on the capacitor, L' is the inductance gradient in the thruster, v is the current sheet speed, x is the instantaneous current sheet axial position, and m is the instantaneous mass in the current sheet. Coaxial electrodes are assumed with constant cross-section (no taper), in which case the inductance gradient is constant[21]

$$L' = \frac{\mu_o}{2\pi} \ln \frac{r_o}{r_i} \ , \tag{6}$$

where μ_o is the permeability of free space, and r_o and r_i are the outer and inner electrode radii, respectively. The instantaneous current sheet mass is calculated using either a slug or snowplow model, as specified by the user. Equations 1-5 were integrated using Matlab.

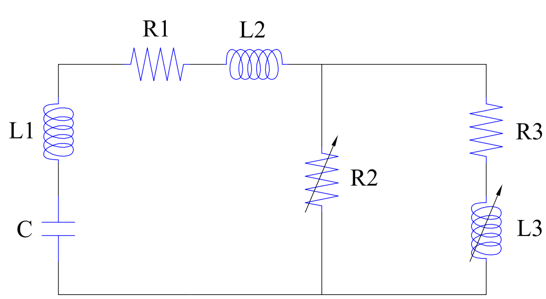

Figure 5: Computational circuit elements of PTC1.

The following circuit parameter values were used to simulate the performance of PRC-PPT1a:

C = 70 μF
R1 = 0 Ω
R2 = 100 Ω
R3 = 2.5×10^{-3} Ω
L1 = 7.5×10^{-9} H
L2 = 20×10^{-9} H

An initial voltage of 37.8 kV was prescribed (E = 50 kJ) with 5 mg of lithium propellant loaded as a slug. The outer electrode radius was set to 10 cm and the inner electrode radius was set to 1 cm (the virtual cathode is assumed to form a thin filament of current along the centerline; a typical current sheet thickness is assumed[13]).

Figure 6 shows the results of the simulation. The current waveform is predicted to be over-damped, reaching a peak of about 1 MA with a pulse length of about 6 μs. The current sheet is predicted to reach a terminal speed of about 110 km/s over about 50 cm of propagation. The total impulse bit derived during a single pulse is estimated to be about 0.6 N-s.

The results of the 0-d model indicate that PRC-PPT1a will use on the order of 5 mg of lithium per pulse, and

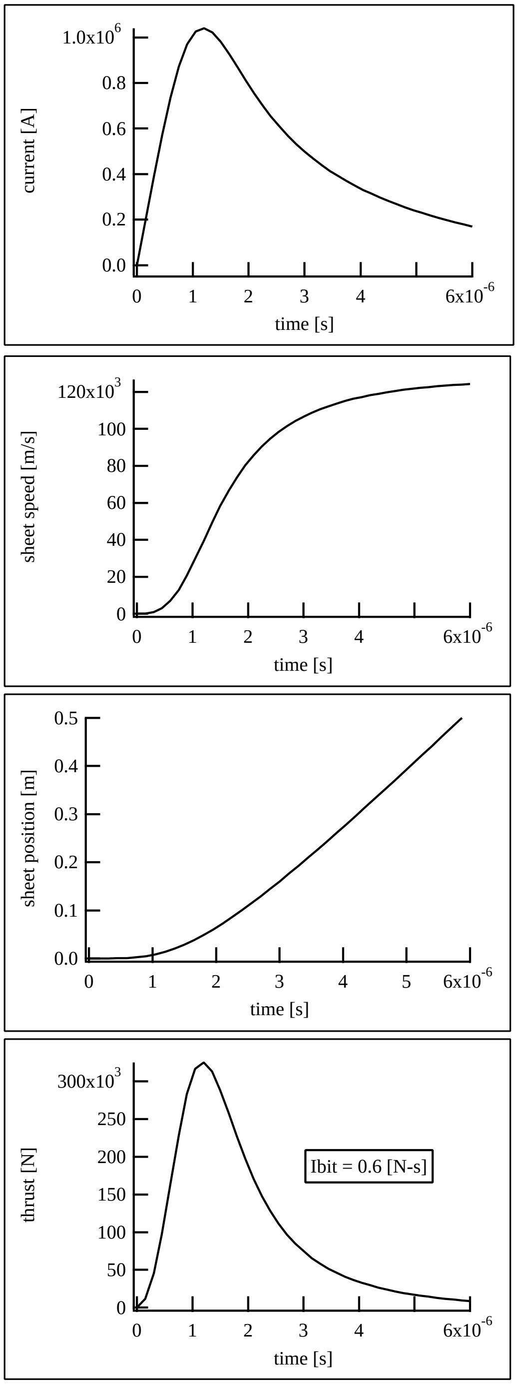

Figure 6: Results of 0-d analysis: current, sheet speed, sheet position, and thrust as a function of time.

require an anode length (L_a) of about 50 cm. The over-simplifications inherent in the 0-d model almost certainly lead to an over-prediction of performance; nevertheless, the results do give us a starting point to begin more sophisticated analysis.

3.2 Lithium droplet decomposition

Based on the results of the 0-d model we can begin to estimate the size of the first stage propellant feed system and capacitor energy requirement.

The density of liquid lithium is 515 kg m^{-3}[22]. Thus, assuming a 5 mg/droplet, the diameter of the lithium droplet which must be introduced into the injector is found to be 2.6 mm.

The energy required to vaporize and (singly)ionize the lithium droplet may be estimated by calculating the number of moles of lithium atoms in a 5 mg sample and multiplying by the heat of vaporization (134.7 kJ/mol) and the ionization energy (513.3 kJ/mol)[22]. The calculation indicates that about 460 J of energy is needed – sizing the first stage capacitor energy to at least 0.5 kJ.

3.3 First stage injection

The injection of the lithium plasma from the first stage into the second stage discharge chamber was modelled using the 2-D MHD code MACH2[23]. A computational mesh which uses the PRC-PPT1a electrode geometry was implemented. The thermal expansion of 5 mg of lithium propellant (1 eV initial temperature) from the inside of the hollow cathode was simulated. The computational mesh and the spatial evolution of the injected plasma at two different times is illustrated in Fig. 7.

The results of the simulation indicate that about ninety percent of the propellant is evacuated from inside the hollow cathode in about 10 μs. In about 12 μs, as illustrated in Fig. 7c, the plasma "reaches" the outer electrode – the second-stage anode. We emphasize the that the term "reaches" is a bit arbitrary; here we have followed the trajectory of the 1 mTorr pressure contour until it contacts the outer electrode, and defined the corresponding time to be the time required for the plasma to bridge the gap.

The use of such a powerful and complicated numerical tool as MACH2 to simulate the first-stage plasma injection may seem to be somewhat of an "overkill". However, we are presently in the process of implementing the electromagnetic and the circuit simulating capabilities of MACH2; the propellant loading illustrated in Fig. 7 will later serve as an initial condition for our full, unsteady MHD simulations.

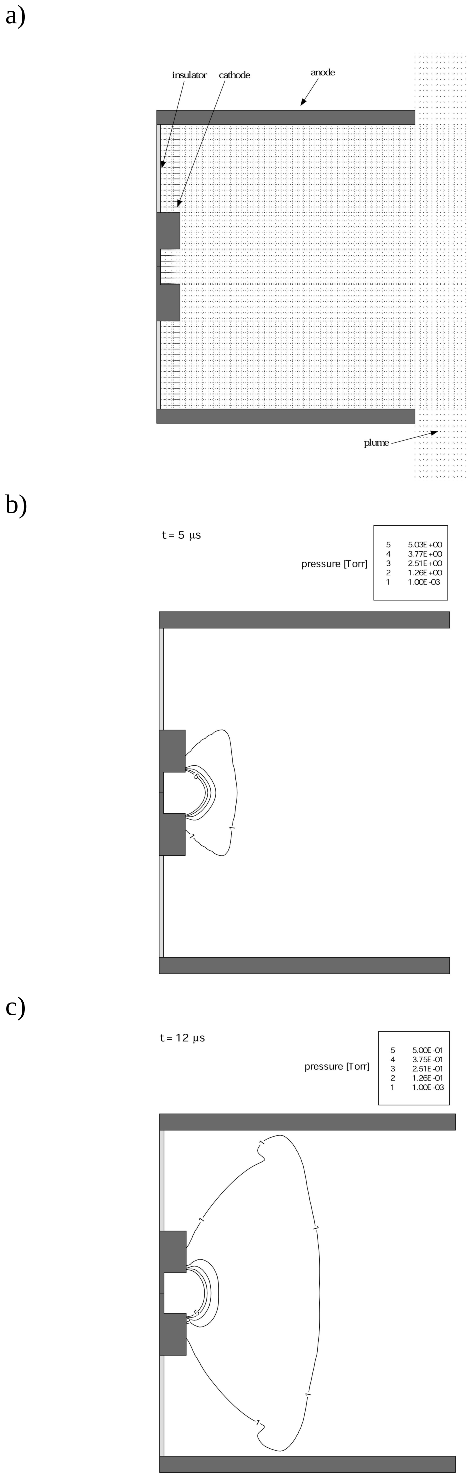

Figure 7: MACH2 injection simulation: a) computational grid layout, b) pressure (t=5 μs), c) pressure (t=12 μs).

4 Conclusion

Design details of a proposed high-energy ($\sim$50 kJ/pulse), two-stage pulsed plasma thruster were presented. The long-term goal of this project is to develop a high-power ($\sim$500 kW), high specific impulse ($\sim$7500 s), highly efficient ($>$50%), and mechanically simple thruster for use as primary propulsion in a high-power nuclear electric propulsion system. The proposed thruster (PRC-PPT1) utilizes a valveless, liquid lithium-fed thermal plasma injector (first stage) followed by a high-energy pulsed electromagnetic accelerator (second stage). A numerical circuit model coupled with one-dimensional current sheet dynamics, as well as a two-dimensional numerical MHD simulation, was used to qualitatively predict the thermal plasma injection and current sheet dynamics, as well as to estimate the projected performance of the thruster. The results of the 0-d circuit model indicate that five milligrams of propellant can be accelerated to 110 km/s in a half-meter long accelerator, using a capacitor bank energy of 50 kJ. While the 0-d code is likely to grossly over-predict the performance of an actual thruster, it provides a starting point to begin more sophisticated analysis.

It is proposed that use of a molten metal propellant and a two-stage acceleration scheme provides potential benefits which may be exploited to overcome many of the negative issues associated with PPTs, such as propellant utilization inefficiency and mechanical reliability. A set of further modelling efforts, and the experimental testing of a prototype thruster, is suggested to determine the feasibility of demonstrating a full scale high-power thruster.

References

[1] J. Marshal. Performance of a hydromagnetic plasma gun. *The Physics of Fluids*, 3(1):134–135, January-February 1960.

[2] R.G. Jahn. *Physics of Electric Propulsion*. McGraw-Hill Book Company, 1968.

[3] K.A. Polzin, E.Y. Choueiri, P. Gurfil, and N.J. Kasdin. Plasma propulsion options for multiple terrestrial planet finder architectures. *Journal of Spacecraft and Rockets*, 39(3):347–356, 2002.

[4] B. Gorowitz, P. Gloersen, and T.W. Karras. Steady state operation of a two-stage pulsed coaxial plasma engine. In 5^{th} *Electric Propulsion Conference*, San Diego, California, March 7-9 1966. AIAA 66-240.

[5] R.G. Jahn K.E. Clark. Quasi-steady plasma acceleration. In *AIAA 7^{th} Electric Propulsion Conference*, Williamsburg, Virginia, March 3-5 1969. AIAA 69-267.

[6] P.J. Turchi and R.L. Burton. Pulsed plasma thruster. *J. Propulsion and Power*, 14(5):716–735, Sept.-Oct. 1998.

[7] J.K. Ziemer, E.A. Cubbin, E.Y. Choueiri, and D. Birx. Performance characterization of a high efficiency gas-fed pulsed plasma thruster. In 33^{rd} *Joint Propulsion Conference*, Seattle, Washington, July 6-9 1997. AIAA 97-2925.

[8] J.K. Ziemer, E.Y. Choueiri, and D. Birx. Is the gas-fed ppt an electromagnetic accelerator? an investigation using measured performance. In 35^{th} *AIAA Joint Propulsion Conference*, Los Angeles, CA, June 20-23 1999. AIAA-99-2289.

[9] J.K. Ziemer and E.Y. Choueiri. Scaling laws for electromagnetic pulsed plasma thrusters. *Plasma Sources Science and Technology*, 10(3):395–405, August 2001.

[10] L.C. Burkhardt and R.H. Lovberg. Current sheet in a coaxial plasma gun. *The Physics of Fluids*, 5(3):341–347, March 1962.

[11] J.W. Berkery and E.Y. Choueiri. Current sheet permeability in electromagnetic pulsed plasma thrusters. In 38^{th} *AIAA Joint Propulsion Conference*, Indianapolis, IN, July 7-10 2002. AIAA-2002-4120.

[12] J.E. Polk. *Mechanisms of Cathode Erosion in Plasma Thrusters*. PhD thesis, Princeton University, 1996.

[13] T.E. Markusic. *Current Sheet Canting in Pulsed Electromagnetic Accelerators*. PhD thesis, Princeton University, 2002.

[14] Y.C.F. Thio, C.E. Knapp, R.C. Kirkpatrick, R.E. Siemon, and P.J. Turchi. A physics exploratory experiment on plasma liner formation. *Journal of Fusion Energy*, (to appear), 2002.

[15] A.V. Larson, T.J. Gooding, B.R. Hayworth, and D.E.T.F. Ashby. An energy inventory in a coaxial plasma accelerator driven by a pulse line energy source. *AIAA Journal*, 3(5):977–979, May 1965.

[16] B.R. Hayworth, T.J. Gooding, and A.V. Larson. A pulse-line energy source for plasma accelerators. In *Fifth Symposium on the Engineering Aspects of Magnetohydrodynamics*, April 1964.

[17] V.P. Ageyev, V.P. Ostrovsky, and V.A. Petrosov. High-current stationary plasma accelerator of high power. In *23^{rd} International Electric Propulsion Conference*, 1993. IEPC-93-117.

[18] P.J. Turchi, C.N. Boyer, and J.F. Davis. Multi-stage plasma propuslion. In *17^{th} International Electric Propulsion Conference*, Tokyo, Japan, May 28-31 1984. IEPC-84-51.

[19] R.D. Alexion, A.R. Keeton, and O.E. Gray III. Demonstration of flow couplers for the lmfbr. In *Progress in Astronautics and Aeronautics*, volume 100, pages 533–547. AIAA, 1985.

[20] J.W. Mather. Formation of a high-density deuterium plasma focus. *The Physics of Fluids*, 8(2):366–377, February 1964.

[21] H. Knoepfel. *Pulsed High Magnetic Fields*. North-Holland Publishing Company, 1970.

[22] J. Emsley. *The Elements*. Oxford University Press, 1998.

[23] R.E. Peterkin Jr. and M.H. Frese. *MACH: A Reference Manual – First Edition*. Air Force Research Laboratory, 1998.